Supplement of Earth Syst. Sci. Data, 14, 3013–3037, 2022
https://doi.org/10.5194/essd-14-3013-2022-supplement

Open Access Earth System Science Data

Supplement of

A 10-year global monthly averaged terrestrial net ecosystem exchange dataset inferred from the ACOS GOSAT v9 XCO_2 retrievals (GCAS2021)

Fei Jiang et al.

Correspondence to: Fei Jiang (jiangf@nju.edu.cn)

Text S1: Method for calculating prior and posterior uncertainties

The posterior and prior uncertainties are calculated based on the prior and posterior perturbations of X_i^b and X_i^a, which are calculated using equation (S1) ~ (S5). X_i^b is perturbed from the prior flux X^b with a Gaussian random distribution δ_i and a set of scaling factors λ. δ_i has a mean of 0 and a standard deviation of 1, and λ represents the uncertainty of each prior flux. After constrained using satellite XCO_2 observations, the perturbed flux of X_i^b is changed to X_i^a according equation (S2) ~ (S5). In these equations, H is the observation operator that maps the state variable from model space to observation space; R is observation error covariance, P^b is the background error covariance; K and $\tilde{K}$ are the Kalman gain matrix of the ensemble mean and ensemble perturbation, respectively. Equation (S2) ~ (S5) are solved in the EnSRF module in our system. In this study, the fluxes are independently perturbed with a spatial resolution of 3°×3°, while X_i^b and X_i^a have a spatial resolution of 1°×1°, that means the fluxes X within each 3° grid have the same perturbation factor ($\lambda \times \delta_i$). In addition, we use a data assimilation window of 1 week, namely the time interval of X_i^b and X_i^a is 1 week.

$$X_i^b = X^b + \lambda \times \delta_i \times X^b \quad , i = 1, 2, \dots, N \tag{S1}$$

$$X_i^a = X^a + (X_i^b - X^b) - \widetilde{\boldsymbol{K}}\boldsymbol{H}(X_i^b - X^b) \tag{S2}$$

$$\widetilde{\boldsymbol{K}} = (1 + \sqrt{\boldsymbol{R}/\boldsymbol{HPH}^T + \boldsymbol{R}})^{-1}\mathbf{K} \tag{S3}$$

$$\boldsymbol{K} = \boldsymbol{PH}^T(\boldsymbol{HPH}^T + \boldsymbol{R})^{-1} \tag{S4}$$

$$\boldsymbol{P} = \frac{1}{n-1}\sum_{i=1}^{n}(X_i^b - X^b)\,(X_i^b - X^b)^T \tag{S5}$$

For the uncertainty σ in a defined region during a time period (monthly or annual), we firstly aggregate each perturbed flux i at each time step t (DA window) to $F_{t,i}$ according to equation (S6), where j is the identifier of grid located in this region, and m is the number of grid in this region. Then, the uncertainty of the regional flux at each time step u_t is given by the standard deviation of $F_{t,I}$ according to equation (S7). Finally, the uncertainty σ during this time period is estimated following equation (S8), where T denotes the time steps within this period.

$$F_{t,i} = \sum_j^m X_{i,j,t} \tag{S6}$$

$$u_t = \sqrt{\frac{1}{N}\sum_{i=1}^{N}(F_{t,i} - \bar{F}_t)^2} \tag{S7}$$

$$\sigma = \sqrt{\sum_{t=1}^{T} u_t \times u_t} \tag{S8}$$

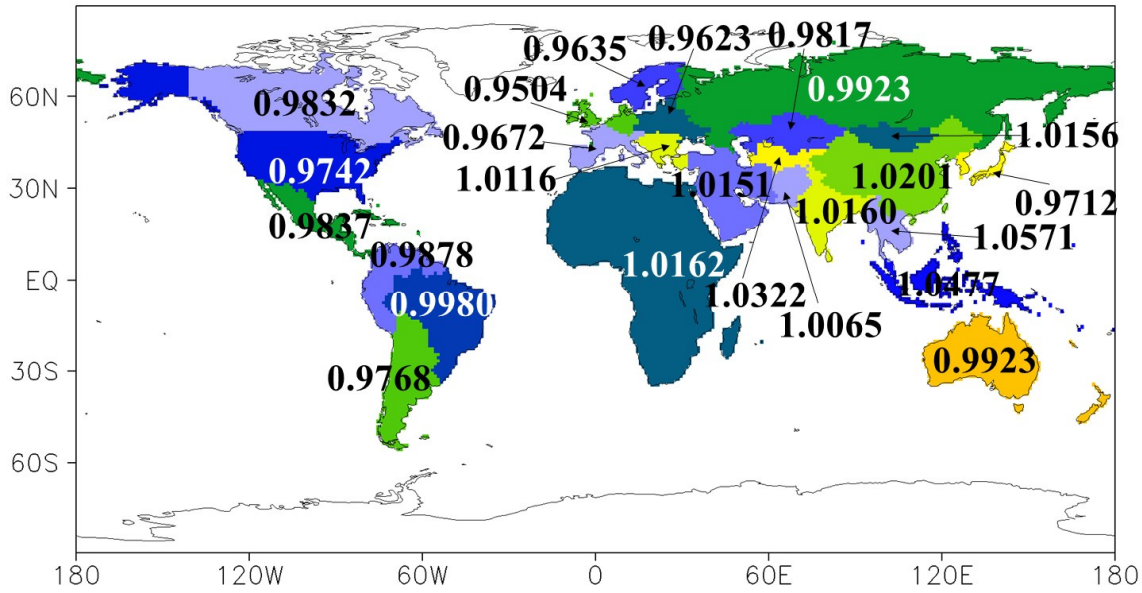

Figure S1: The change rate of fossil fuel and cement carbon emissions in each region in 2019 compared with 2018

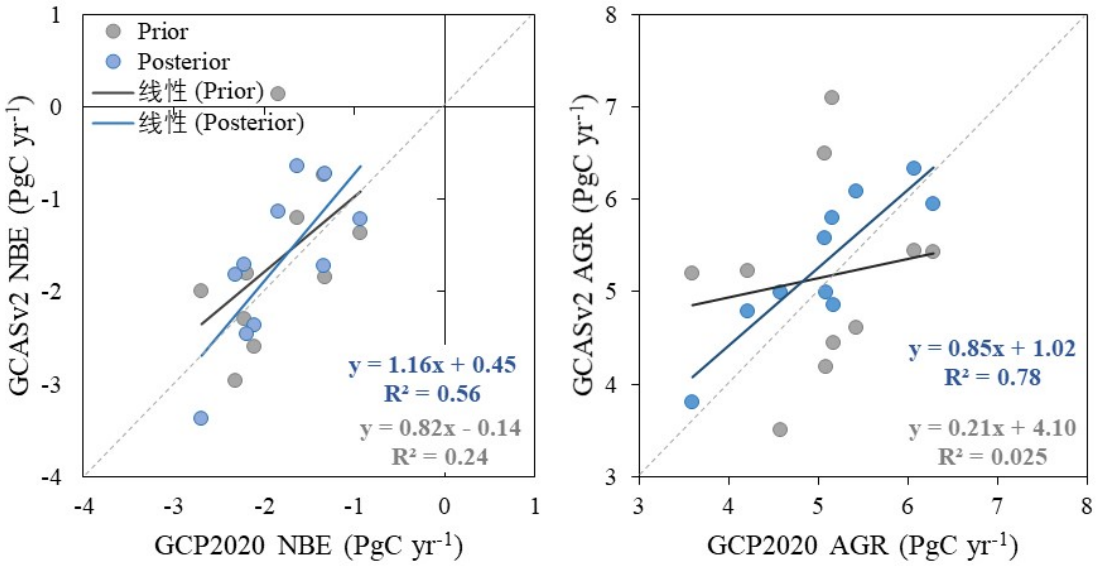

Figure S2: Comparisons between this study and GCP2020 for the estimates of annual (a) NBE and (b) AGR from 2010 to 2019

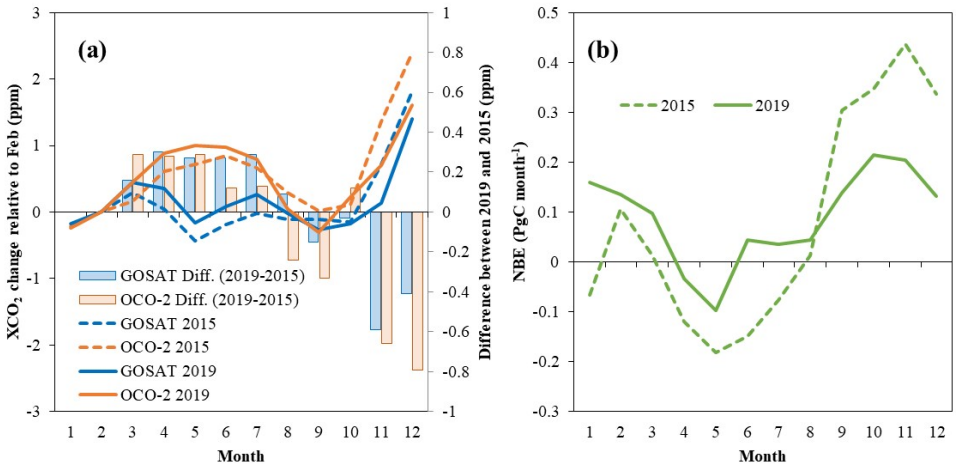

Figure S3: Monthly variations of (a) XCO_2 and (b) NBE in tropical latitudes (TL, 30° S ~ 30° N) in 2015 and 2019 (because GOSAT lacks data in January 2015, XCO_2 for each month is its change relative to February. It could be found that the carbon sinks in January-August and September-December 2019 were significantly smaller and stronger than those in the same period in 2015, respectively. Correspondingly, compared with 2015, GOSAT has higher XCO_2 in March - August, and lower ones in September-December in 2019. Although OCO-2 has a similar pattern, compared with 2015, the XCO_2 increase in March-August is significantly smaller than that of GOSAT, while the decrease in September-December is significantly higher than that of GOSAT. The annual mean GOSAT XCO_2 in 2019 is higher than that in 2015, while OCO-2 is the opposite)

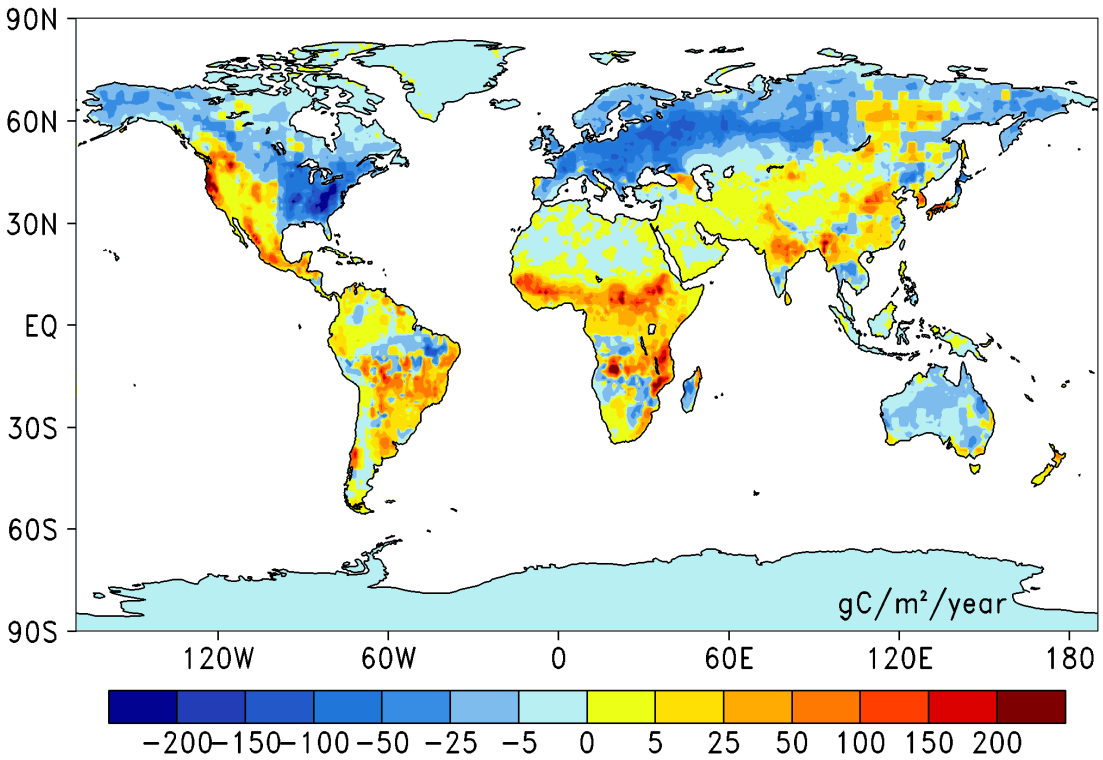

Figure S4: Global distributions of the mean differences between the prior and posterior NEE averaged from 2010 to 2019

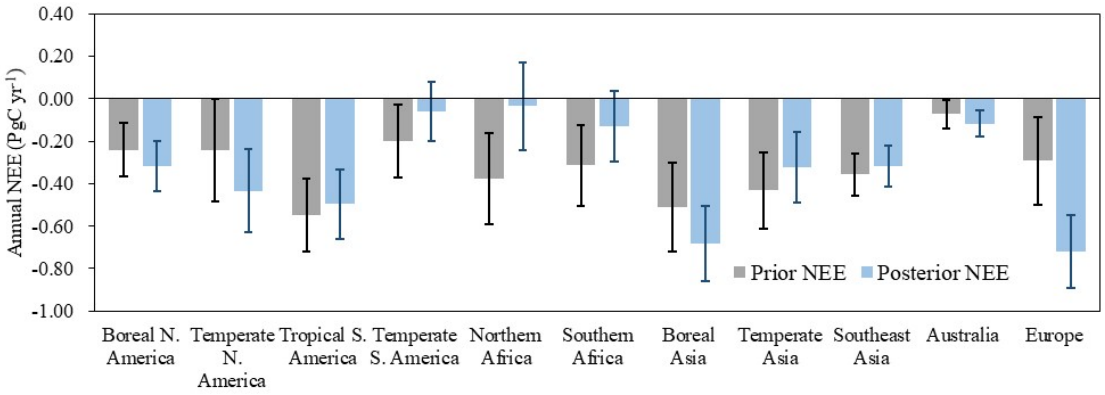

Figure S5: Differences between the prior and posterior NEE in each TRANSCOM 3 regions

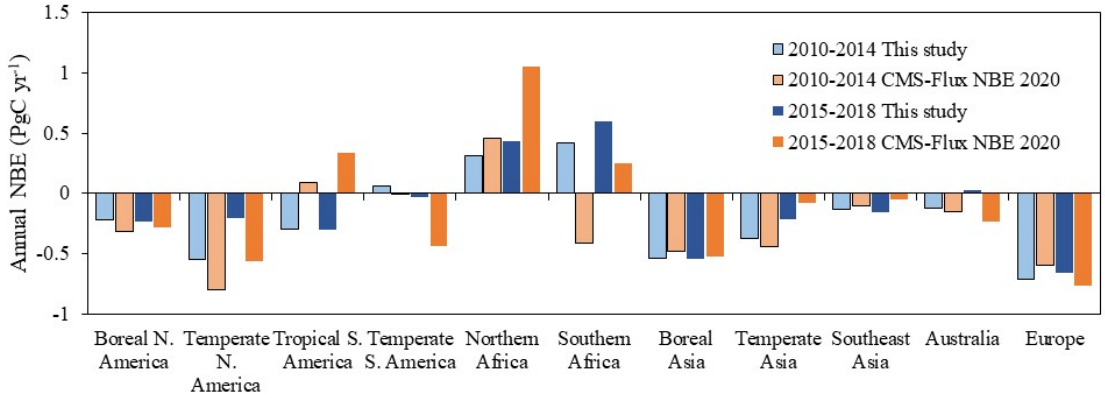

Figure S6: Comparison of NBE between this study and CMS-Flux NBE 2010 for the periods of 2010-2014 and 2015-2018

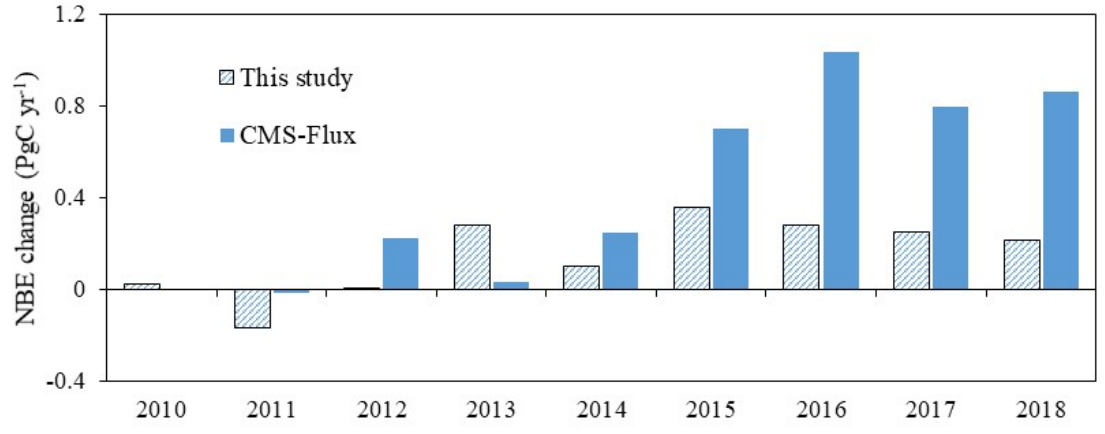

Figure S7: Changes in posterior NBE relative to prior fluxes in southern Africa (positive means source increase)

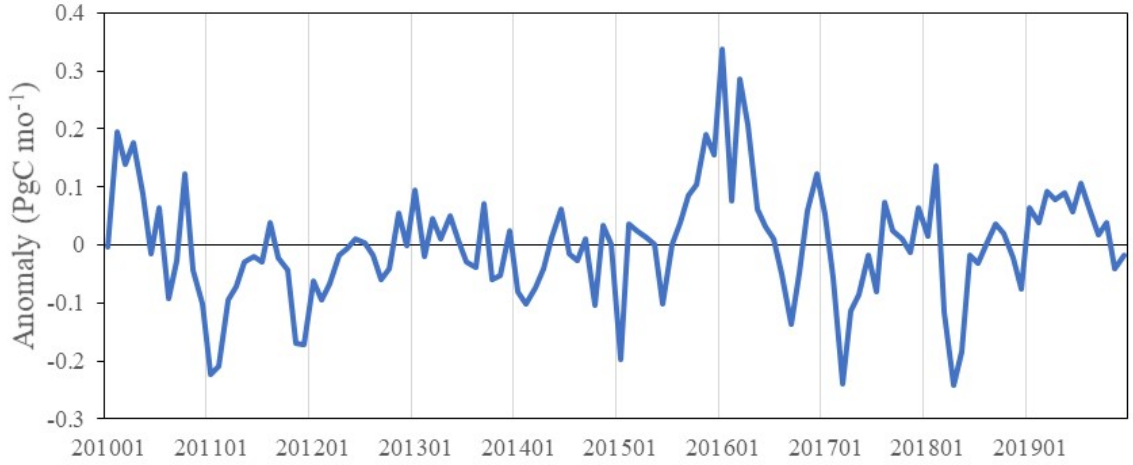

Figure S8: Anomaly of monthly NEE in the pantropical area (30°S ~ 30°N)

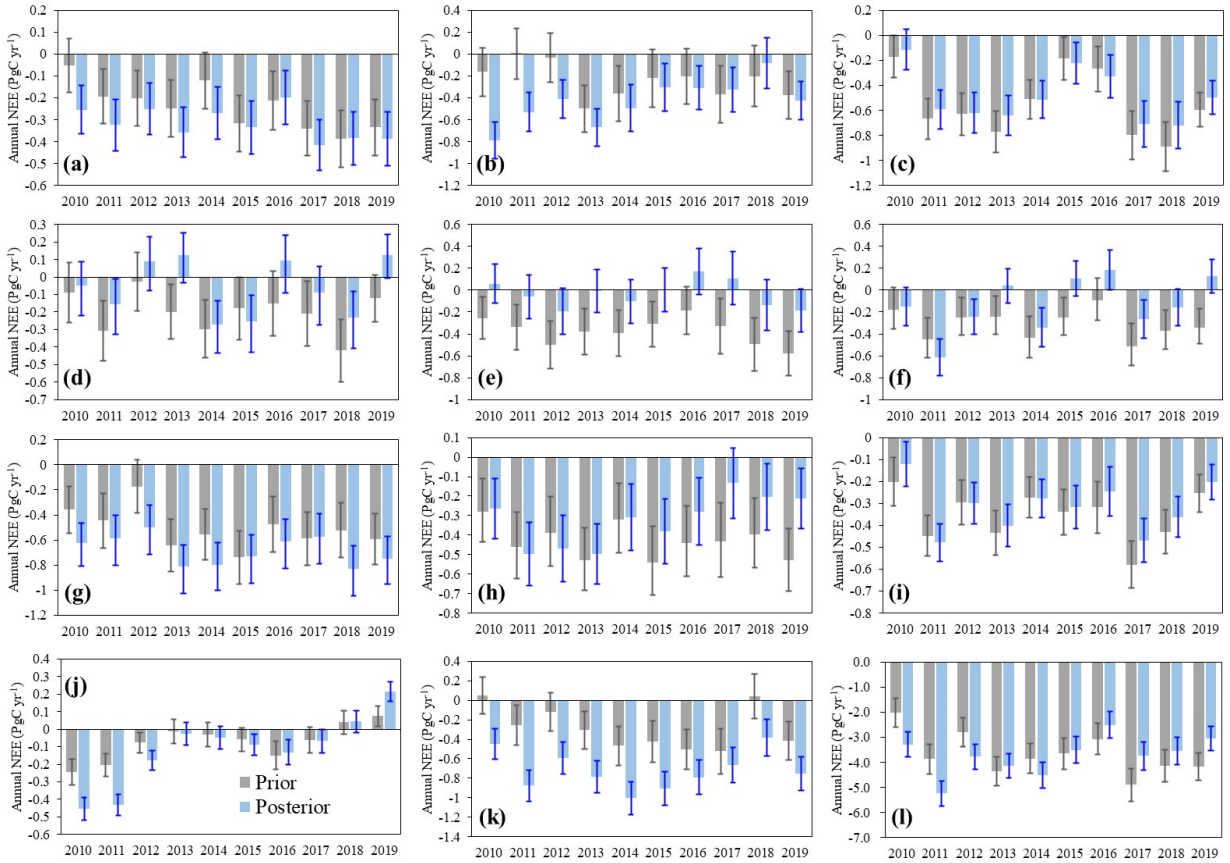

Figure S9: Interannual variations of the prior and posterior NEE in each TRANSCOM 3 region and in the global scale. (a, Boreal North America; b, Temperate North America; c, Tropical South America; d, Temperate South America; e, Northern Africa; f, Southern Africa; g, Boreal Asia; h, Temperate Asia; i, Southeast Asia; j, Australia; k, Europe; l, Globe)

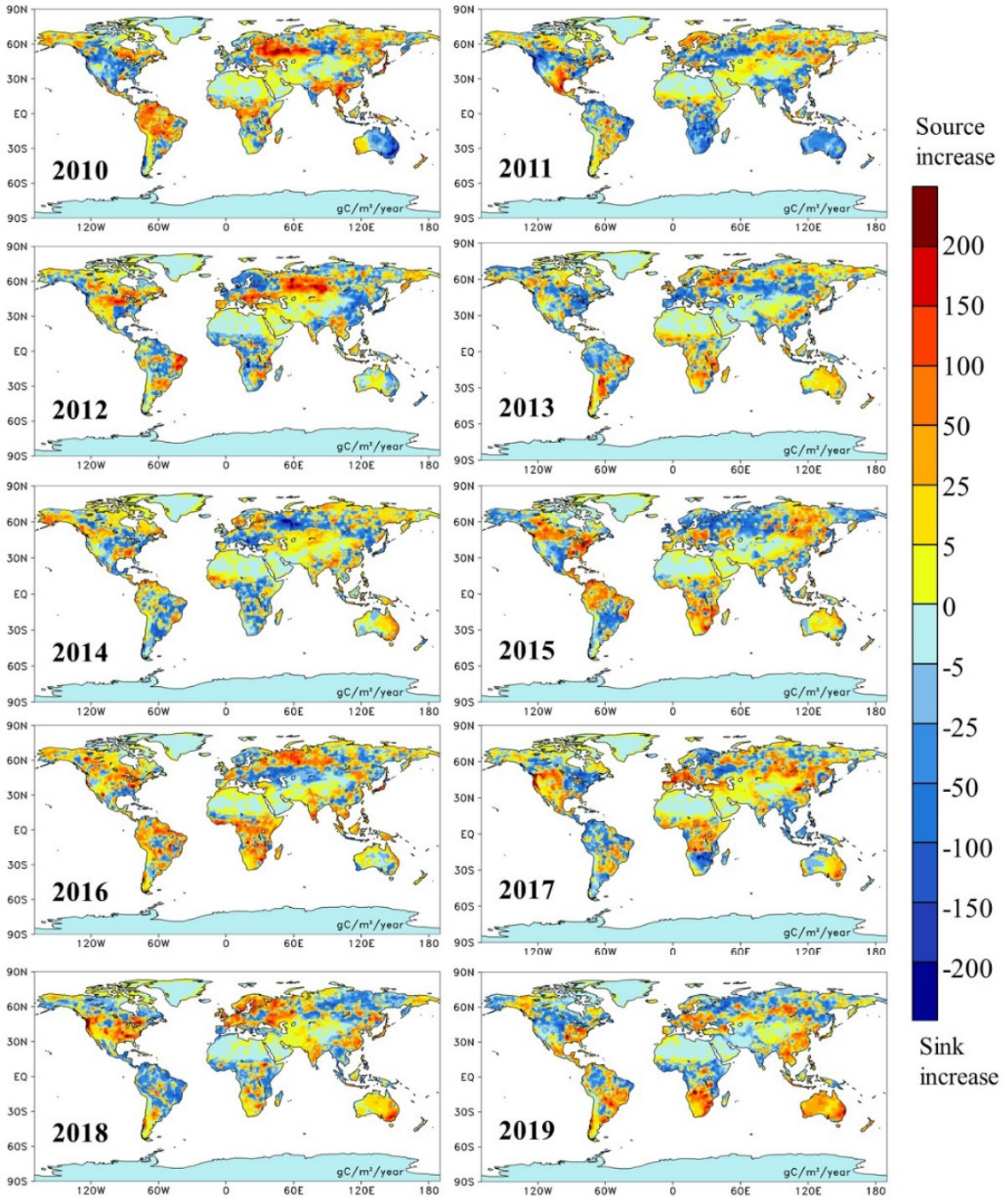

Figure S10: The spatial patterns of NEE anomaly in each year (gC m^{-2} yr^{-1})

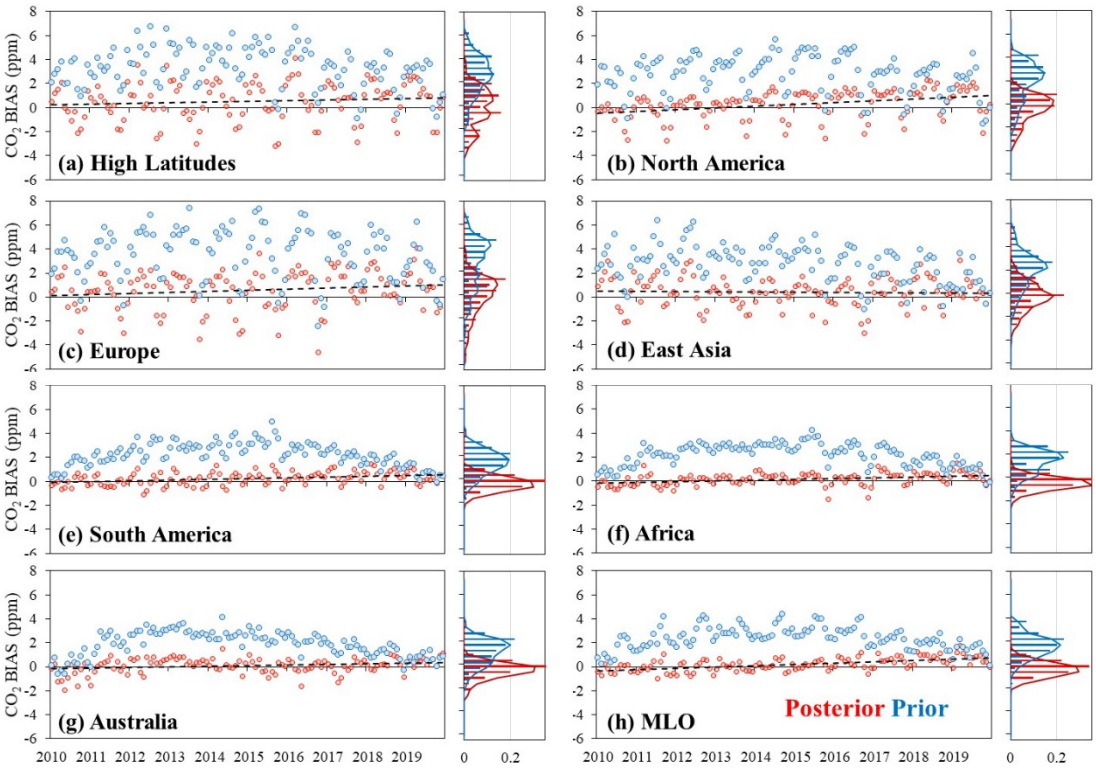

Figure S11: Time series of monthly averaged biases between observations and simulations and the frequency distribution of the biases in the 7 regions and MLO site (the black dotted line represents the linear trend of the biases between the observations and the posterior simulations)

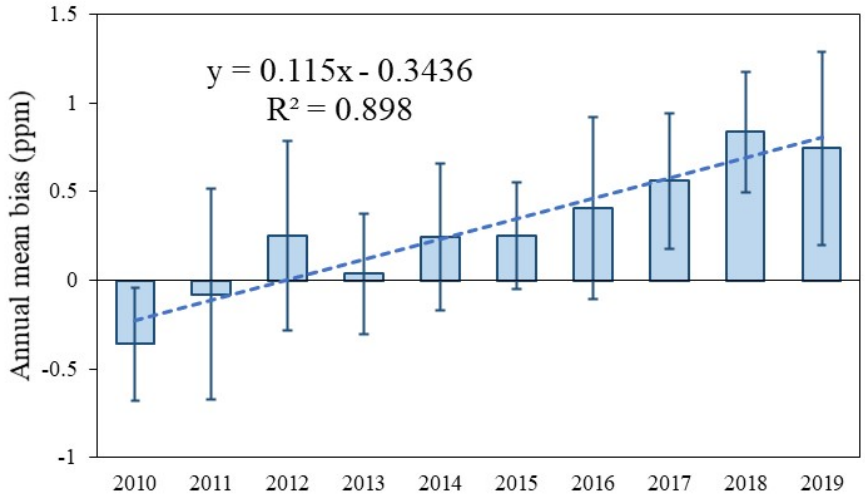

Figure S12: Inter-annual variations of the global averaged annual mean bias (error bar represents standard deviation of monthly mean biases in one year; the dotted line is its linear trend)

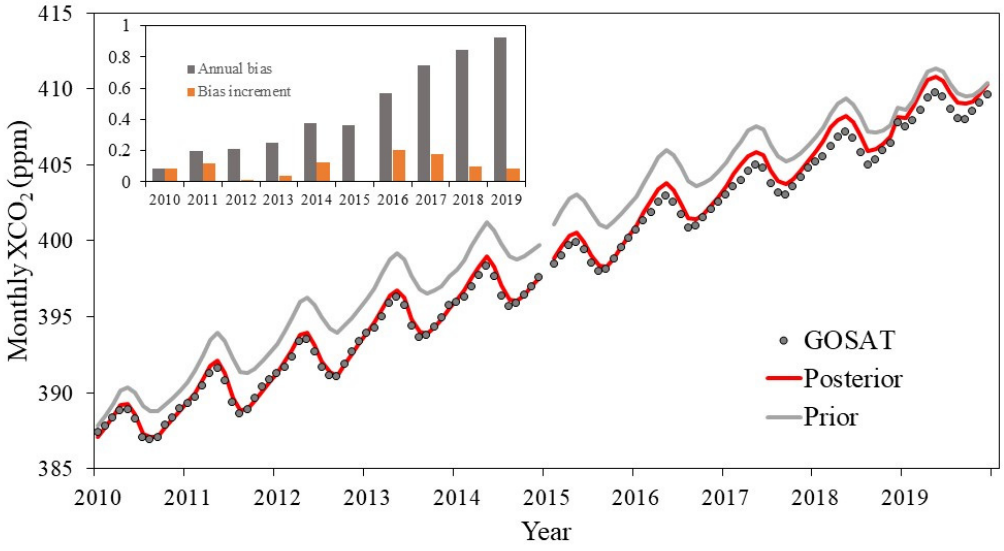

Figure S13: Global mean monthly XCO_2 from 2010 to 2019 (the small figure shows the annual mean biases and bias increment in each year)

Table S1: Information of the selected surface flask observations and the evaluation results

Locations	Site	Lab id	Lat	Lon	BIAS	MAE	RMSE	CORR	No. of data
High latitudes	alt	1	82.45	297.49	0.7	1.54	2.07	0.98	518
	brw	1	71.32	203.39	0.29	2	2.61	0.97	555
	crv	1	64.99	212.4	0.47	2.79	3.52	0.93	1260
	ice	1	63.4	339.71	0.56	1.63	2.01	0.96	161
	pal	1	67.97	24.12	-0.04	2.53	3.34	0.96	438
	sum	1	72.6	321.58	0.35	1.27	1.54	0.99	506
	tik	1	71.6	128.89	0.96	3.11	4.03	0.94	303
	zep	1	78.91	11.89	0.88	1.83	2.44	0.97	500
North America	amt	1	45.03	291.32	1.97	3.26	4.07	0.95	1356
	bao	1	40.05	255	-0.8	2.49	3.28	0.86	1754
	bmw	1	32.26	295.12	1.69	1.99	2.58	0.97	397
	hsu	1	41.03	235.65	-0.24	2.67	3.46	0.9	69
	inx	1	39.8	273.98	0.51	3.79	4.66	0.93	409
	key	1	25.67	279.84	0.49	1.65	2.38	0.96	413
	lef	1	45.95	269.73	0.69	3	3.8	0.95	1611
	mbo	1	43.98	238.31	0.15	1.59	2.11	0.96	1500
	mex	1	18.98	262.69	0.97	1.27	1.66	0.98	387
	mwo	1	34.22	241.94	-0.81	2.24	3.11	0.92	3185
	nwr	1	40.05	254.41	0.06	1.6	2.15	0.96	489
	sct	1	33.41	278.17	0.47	3.22	4.05	0.93	1689
	sgp	1	36.61	262.51	0.72	3.28	3.99	0.93	437
	str	1	37.76	237.55	0.05	2.35	3.09	0.94	4842
	thd	1	41.05	235.85	-1.05	2.35	3.13	0.91	330
	uta	1	39.9	246.28	1.5	2.54	3.23	0.94	462
	wbi	1	41.72	268.65	1.33	3.43	4.32	0.94	1645
	wgc	1	38.26	238.51	-0.09	3.34	4.14	0.9	1238
	wkt	1	31.31	262.67	0.58	2.47	3.2	0.93	1326
Europe	bgu	11	41.97	3.23	-0.3	2.74	3.45	0.92	223
	cib	1	41.81	355.07	0.35	2.99	3.72	0.92	406
	fkl	11	35.34	25.67	0.49	2.41	2.97	0.94	207
	hpb	1	47.8	11.02	2.61	4.3	5.04	0.92	394
	hun	1	46.95	16.65	0.65	3.62	4.42	0.94	426
	lmp	1	35.52	12.62	0.58	1.91	2.4	0.96	415
	mhd	1	53.33	350.1	0.2	1.52	2.15	0.97	474
	oxk	1	50.03	11.81	-0.13	3.3	4.07	0.91	360
	pdm	11	42.94	0.14	-0.44	1.82	2.35	0.95	170
East Asia	dsi	1	20.7	116.73	0.87	2.29	2.92	0.94	376
	lln	1	23.47	120.87	1.06	2.33	3.15	0.95	384
	tap	1	36.74	126.13	1.52	3.5	4.41	0.92	411
	uum	1	44.45	111.1	-0.41	2.79	3.57	0.93	453

	wlg	1	36.29	100.9	-0.45	1.89	2.62	0.95	477
South America	nat	1	-5.8	324.81	0.11	1.09	1.52	0.97	331
	rpb	1	13.16	300.57	0.36	0.72	0.95	0.99	511
	ush	1	-54.85	291.69	0.24	0.64	0.88	0.99	206
Africa	ask	1	23.26	5.63	0.01	0.65	0.83	1	474
	cpt	1	-34.35	18.49	0.53	0.66	0.9	0.99	241
	nmb	1	-23.58	15.03	-0.11	0.78	1.09	0.99	403
	sey	1	-4.68	55.53	0.57	0.81	1.2	0.99	416
	wis	1	29.96	35.06	0.17	1.98	2.57	0.95	479
Australia	bhd	1	-41.41	174.87	-0.01	0.71	1.13	0.99	144
	cfa	2	-19.28	147.06	-0.03	0.92	1.27	0.99	176
	cgo	1	-40.68	144.69	0.02	0.46	0.82	0.99	337
	gpa	2	-12.25	131.04	1.29	2.23	2.71	0.92	64
	asc	1	-7.97	345.6	0.57	0.73	0.91	1	836
	azr	1	38.77	332.62	0.29	1.57	2.02	0.96	218
	cba	1	55.21	197.28	-0.91	2.08	2.82	0.96	808
	chr	1	1.7	202.85	0.59	0.85	1.07	0.99	249
	crz	1	-46.43	51.85	0.1	0.32	0.41	1	396
	cya	2	-66.28	110.52	0.24	0.31	0.39	1	222
	eic	1	-27.16	250.57	0.16	0.91	1.39	0.98	342
	gmi	1	13.39	144.66	0.41	1.07	1.58	0.98	525
	hba	1	-75.61	333.79	0.34	0.4	0.47	1	323
	izo	1	28.31	343.5	0.59	1.06	1.44	0.99	483
	kum	1	19.56	205.11	-0.18	1.25	1.79	0.98	718
	maa	2	-67.62	62.87	0.36	0.38	0.46	1	239
	mid	1	28.21	182.62	0.54	1.34	1.73	0.98	465
	mlo	1	19.54	204.42	0.22	0.61	0.8	1	637
	mqa	2	-54.48	158.97	0.17	0.4	0.55	1	242
	psa	1	-64.92	296	0.21	0.38	0.47	1	466
	rk1	426	-29.2	182.1	-0.07	0.58	0.7	1	49
	shm	1	52.71	174.13	-0.2	2.07	2.76	0.96	429
	smo	1	-14.25	189.44	0.37	0.57	0.76	1	798
	spo	1	-89.98	335.2	0.3	0.35	0.41	1	494
	syo	1	-69.01	39.59	0.28	0.34	0.4	1	237
		All			0.35	1.76	2.28	0.96	-